



OPEN

## Continuous and non-invasive thermography of mouse skin accurately describes core body temperature patterns, but not absolute core temperature

Vincent van der Vinne<sup>1,5</sup>✉, Carina A. Pothecary<sup>2</sup>, Sian L. Wilcox<sup>1</sup>, Laura E. McKillop<sup>1</sup>, Lindsay A. Benson<sup>2</sup>, Jenya Kolpakova<sup>3</sup>, Shu K. E. Tam<sup>2</sup>, Lukas B. Krone<sup>1</sup>, Angus S. Fisk<sup>2</sup>, Tatiana S. Wilson<sup>2</sup>, Tomoko Yamagata<sup>2</sup>, James Cantley<sup>4</sup>, Vladyslav V. Vyazovskiy<sup>1</sup> & Stuart N. Peirson<sup>1,2</sup>✉

Body temperature is an important physiological parameter in many studies of laboratory mice. Continuous assessment of body temperature has traditionally required surgical implantation of a telemeter, but this invasive procedure adversely impacts animal welfare. Near-infrared thermography provides a non-invasive alternative by continuously measuring the highest temperature on the outside of the body ( $T_{\text{skin}}$ ), but the reliability of these recordings as a proxy for continuous core body temperature ( $T_{\text{core}}$ ) measurements has not been assessed. Here,  $T_{\text{core}}$  (30 s resolution) and  $T_{\text{skin}}$  (1 s resolution) were continuously measured for three days in mice exposed to ad libitum and restricted feeding conditions. We subsequently developed an algorithm that optimised the reliability of a  $T_{\text{skin}}$ -derived estimate of  $T_{\text{core}}$ . This identified the average of the maximum  $T_{\text{skin}}$  per minute over a 30-min interval as the optimal way to estimate  $T_{\text{core}}$ . Subsequent validation analyses did however demonstrate that this  $T_{\text{skin}}$ -derived proxy did not provide a reliable estimate of the absolute  $T_{\text{core}}$  due to the high between-animal variability in the relationship between  $T_{\text{skin}}$  and  $T_{\text{core}}$ . Conversely, validation showed that  $T_{\text{skin}}$ -derived estimates of  $T_{\text{core}}$  reliably describe temporal patterns in physiologically-relevant  $T_{\text{core}}$  changes and provide an excellent measure to perform within-animal comparisons of relative changes in  $T_{\text{core}}$ .

Body temperature is a key physiological parameter that affects a host of physiological processes and can be utilised as a scientific and humane endpoint in biomedical research<sup>1–4</sup>. Despite its physiological relevance, body temperature is often ignored in rodent studies because of the practical difficulties associated with its measurement; especially when continuous measurements are required.

The measurement of body temperature in small rodents is typically performed by contact method, implanted telemeter or thermal imaging<sup>5</sup>. Each of these methods is associated with pros and cons<sup>5</sup>. Contact measurements such as inserting a rectal temperature probe are relatively easy to perform and do not require expensive equipment but are associated with an increased body temperature due to handling stress for the animal, potential health complications due to probe insertion, and only provide a snapshot of a continuously changing variable. Telemeter implantation enables the continuous and accurate recording of core body temperature ( $T_{\text{core}}$ ) but requires invasive surgery resulting in stress, may alter physiology, requires substantial time and skill from the researcher, and malfunctions of the telemeter can typically not be remedied. Thermal imaging and other non-contact temperature measurements provide a non-invasive method to record body temperature<sup>6</sup>, but these

<sup>1</sup>Department of Physiology and Genetics, Sleep and Circadian Neurosciences Institute, University of Oxford, Oxford, UK. <sup>2</sup>Nuffield Department of Clinical Neurosciences, Sleep and Circadian Neurosciences Institute, University of Oxford, Oxford, UK. <sup>3</sup>Department of Neurobiology, Brudnick Neuropsychiatric Research Institute, University of Massachusetts Medical School, Worcester, MA, USA. <sup>4</sup>Division of Systems Medicine, School of Medicine, University of Dundee, Dundee, UK. <sup>5</sup>Department of Biology, Williams College, Williamstown, MA, USA. ✉email: vv5@williams.edu; stuart.peirson@eye.ox.ac.uk

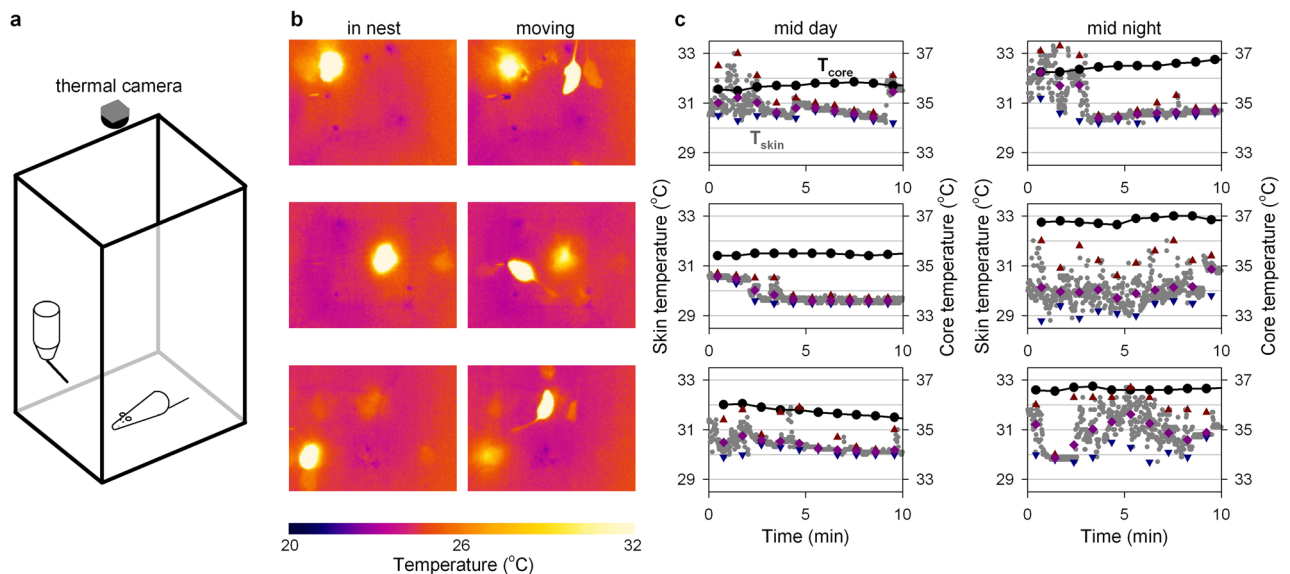


**Figure 1.** Continuous recording of skin ( $T_{skin}$ ) and core temperature ( $T_{core}$ ) in freely-moving laboratory mice. (a) Mice were each individually housed in an open-topped cage placed under a thermal camera. (b) Thermal images of three mice at rest (left) and while moving through the cage (right). Skin temperature was recorded by storing the temperature of the warmest pixel in view (1 Hz). (c) Representative 10-min traces of  $T_{core}$  (1  $\text{min}^{-1}$ , black dots) and  $T_{skin}$  (1 Hz, grey dots) for three mice in the middle of the light- (left) and dark-phase (right). The distribution of  $T_{skin}$  measurements within each minute is quantified by the minimal (blue), mean (pink) and maximal (red)  $T_{skin}$ . Large fluctuations in  $T_{skin}$  can be observed especially at night, likely as a result of variability in the warmest observed pixel due to movement of the animal.

methods typically require animal handling, are not continuous, and do not measure  $T_{core}$ <sup>7–18</sup>. The non-invasive nature of thermography measurements does however provide the potential to assess body temperature in undisturbed freely-moving laboratory mice, removing the confounding factor of handling stress and representing an obvious refinement in terms of animal welfare.

Here, we develop and optimise an algorithm for processing thermal imaging data of freely-moving mice with the goal of assessing whether the resulting  $T_{core}$  estimate, based on continuous measurements of the highest temperature on the outside of the body ( $T_{skin}$ ), can be used to describe (changes in)  $T_{core}$ . Mice were implanted intraperitoneally with a body-temperature telemeter while  $T_{skin}$  was recorded every second by thermal imaging for three days. This was done under standard laboratory conditions as well as in a subgroup of food-restricted mice exhibiting daily torpor, a transient hypometabolic state associated with a marked decrease in body temperature<sup>3</sup>. Assessment of different algorithm parameters (summary statistics, sampling and averaging intervals) identified averaging of the maximum  $T_{skin}$  per 60 s over 30-min intervals ( $T_{skin,max}$ ) as the most reliable way to estimate  $T_{core}$ .  $T_{skin,max}$  provides an accurate description of relative changes in  $T_{core}$  within individual animals. Between-animal variation in the relationship between  $T_{core}$  and  $T_{skin,max}$  does however limit the utility of  $T_{skin}$  measurements as a measure of absolute within-animal changes in  $T_{core}$  or differences in  $T_{core}$  between animals.

## Results

### Estimating core body temperature non-invasively by continuously recording skin temperature.

Measuring  $T_{skin}$  using near-infrared thermography enables the continuous assessment of body temperature during both day and night in freely-moving animals. Here,  $T_{skin}$  was recorded in five wildtype mice housed in open-topped cages at an ambient temperature of  $22 \pm 1$  °C (Fig. 1a). A limited amount of nesting material was provided, to ensure that the mice were fully visible at all times. As expected, the warmest spot in each image was associated with the location of the mouse in the cage (Fig. 1b), thus enabling the description of  $T_{skin}$  by recording the temperature of the warmest pixel each second (Fig. 1c). As illustrated in the representative 10-min recordings (Fig. 1c),  $T_{skin}$  often changed rapidly ( $< 1$  min) by 1–2 °C while the simultaneously recorded  $T_{core}$  did not reveal corresponding changes. Based on observations of the mice during these recordings, we established that these rapid changes in  $T_{skin}$  were typically associated with movement of the animal. The observed  $T_{skin}$  was typically higher and more variable during movement, likely as a result of changes in the exposed parts of the skin due to the animal's change in position and posture (Fig. S1). Consistent with this interpretation, periods of high  $T_{skin}$  variability were more common during the night when mice are most active. The high variability of  $T_{skin}$  compared to  $T_{core}$  (Fig. 1c) highlights the importance of processing  $T_{skin}$  measurements to obtain a reliable proxy for  $T_{core}$  rather than relying on raw  $T_{skin}$  measurements.

**Reducing skin temperature variability by optimising algorithm parameters.** The algorithm developed here was designed to estimate  $T_{core}$  based on  $T_{skin}$  measurements taken every second. For this, a summary statistic was used to describe  $T_{skin}$  during each short sampling interval (1 s–10 min) and these values

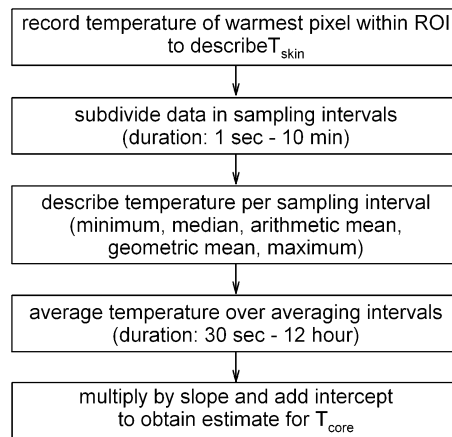


**Figure 2.** Dataflow used to optimise the estimation of  $T_{\text{core}}$  based on  $T_{\text{skin}}$  measurements.

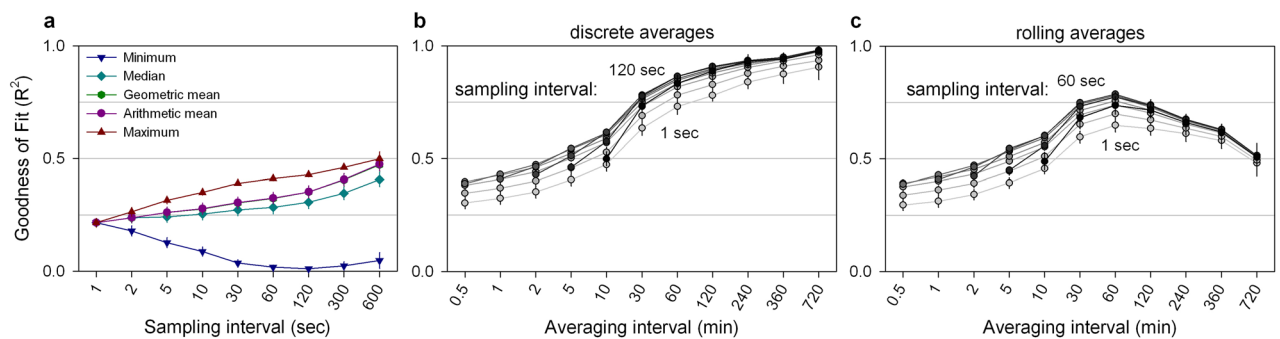


**Figure 3.** Optimisation of algorithm parameters used to estimate  $T_{\text{core}}$  based on thermal camera measurements of  $T_{\text{skin}}$ . **(a)** Goodness of fit associated with different summary statistics calculated over intervals between 1 s and 10 min. The outcomes associated with the arithmetic mean and geometric mean are indistinguishable. **(b)** Goodness of fit associated with discrete estimates of  $T_{\text{core}}$  for each averaging-interval duration based on  $T_{\text{skin,max}}$  over different sampling intervals (1–600 s) and averaged over intervals between 30 s and 12 h. Fill and line colour become progressively darker with increasing sampling interval duration. Sampling of  $T_{\text{skin,max}}$  over intermediate sampling intervals (30–120 s) consistently resulted in a better description of  $T_{\text{core}}$  compared to shorter and longer sampling intervals. Sampling  $T_{\text{skin,max}}$  over an intermediate sampling interval resulted in an ~15% improvement of fit compared to taking the mean temperature (i.e. 1 s sampling interval) over the same averaging interval. **(c)** Goodness of fit associated with estimating each measurement of  $T_{\text{core}}$  (30 s time resolution) using a rolling average based on  $T_{\text{skin,max}}$  over different sampling intervals (1–600 s) and averaged over intervals between 30 s and 12 h. Fill and line colour become progressively darker (lightest: 1 s → darkest: 600 s) with increasing sampling interval duration. Data represents the between-individual mean and SEM goodness of fit associated with the presented combination of algorithm parameters.

were averaged over a longer averaging interval (30 s–12 h). This averaged measure of  $T_{\text{skin}}$  ( $T_{\text{skin,max}}$ ) was subsequently transformed to obtain an estimate of  $T_{\text{core}}$  using the slope and intercept describing the linear relationship between  $T_{\text{skin,max}}$  and  $T_{\text{core}}$  (Fig. 2). The present paper describes the optimisation of algorithm parameters with the objective of estimating  $T_{\text{core}}$  with high accuracy, equal variance at different levels of  $T_{\text{core}}$ , and ideally a relationship between  $T_{\text{skin,max}}$  and  $T_{\text{core}}$  with a slope of 1 (i.e.  $T_{\text{core}} = T_{\text{skin,max}} + \text{constant}$ ).

The optimal algorithm parameters were determined by assessing how the possible parameter combinations (sampling interval, summary statistic, averaging interval) affected the reliability of the  $T_{\text{core}}$  estimate. The optimal sampling interval and summary statistic for estimating  $T_{\text{core}}$  based on  $T_{\text{skin}}$  measurements was determined by comparing the goodness of fit associated with each combination of algorithm parameters (Fig. 3a). Using the minimal  $T_{\text{skin}}$  per sampling interval to estimate  $T_{\text{core}}$  resulted in a progressively worse fit with increasing sampling interval length while all other summary statistics resulted in an improved fit with longer sampling intervals. In all five mice, use of the maximum temperature as a summary statistic resulted in a better fit of  $T_{\text{core}}$  compared to the median, arithmetic- or geometric mean, especially at intermediate sampling interval lengths (Fig. 3a, Fig. S2). The superiority of using the maximum per sampling interval as opposed to calculating the arithmetic mean over the whole averaging interval is illustrated in subsequent analyses (Fig. 3b,c) by the improved goodness of fit associated with different sampling intervals compared to the 1-s interval (since the  $T_{\text{skin}}$  sampling rate was also 1 s, the 1-s sampling interval estimate is equivalent to taking the mean over all measurements within

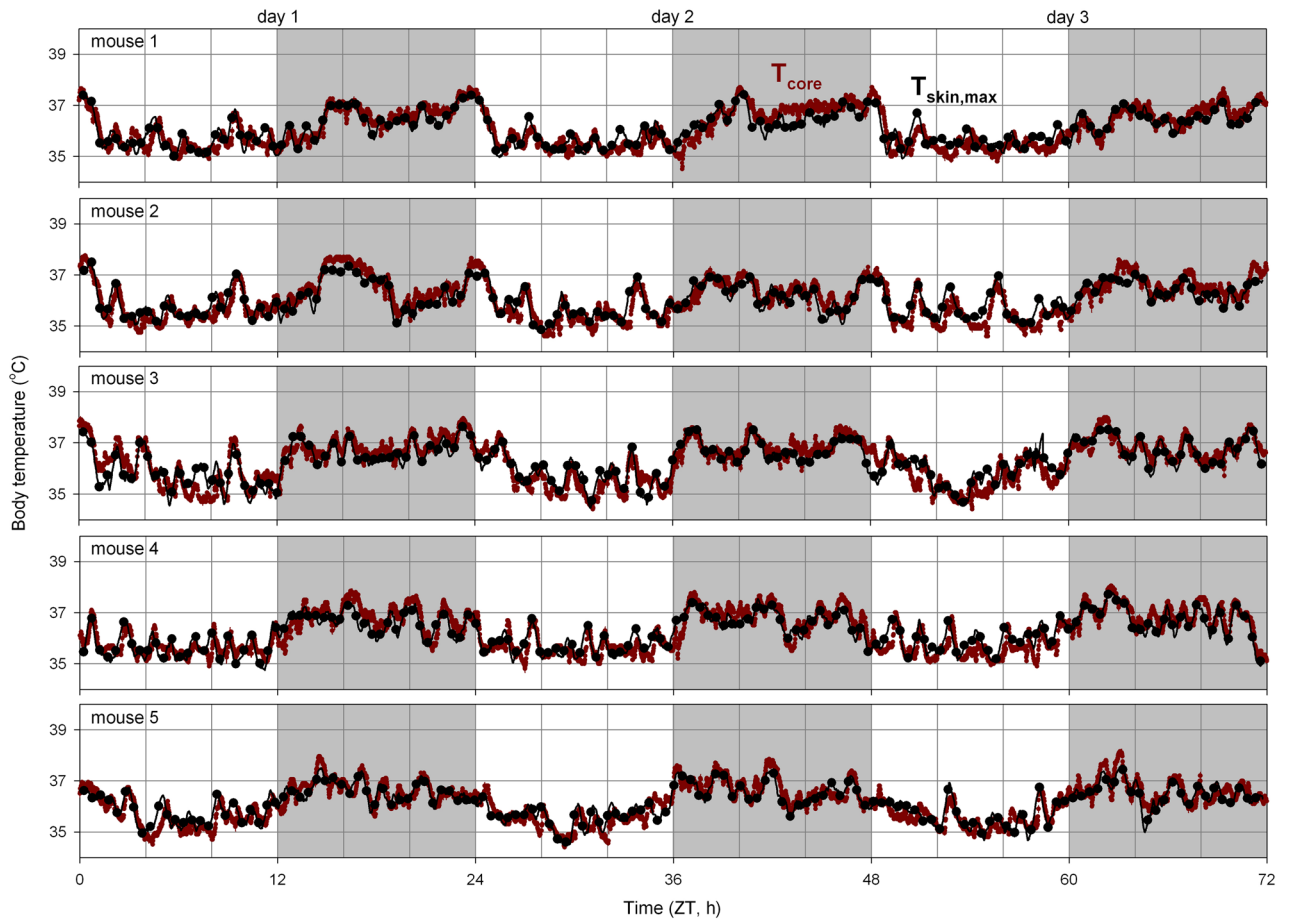


**Figure 4.** Three-day core temperature recordings measured directly ( $T_{\text{core}}$ , red) and estimated based on skin temperature ( $T_{\text{skin,max}}$ , black) in five mice. Core temperature estimates based on  $T_{\text{skin,max}}$  are depicted as a rolling average (black line) and as discrete averages (black dots, 1 per 30 min).  $T_{\text{skin,max}}$  was calculated by averaging the maximum  $T_{\text{skin}}$  per minute over a 30-min interval. Slope and intercept describing the linear relationship between  $T_{\text{skin,max}}$  and  $T_{\text{core}}$  were optimised for each mouse individually. Day and night are represented by the white- and light-grey background, respectively. As expected for a nocturnal species, both  $T_{\text{core}}$  and  $T_{\text{skin,max}}$  measurements show that body temperature is highest during the night in mice. ZT: Zeitgeber time.

an averaging interval). The optimal sampling interval also depended on the chosen averaging interval with sampling intervals of 60 s or 120 s resulting in the best estimate of  $T_{\text{core}}$  while both shorter and longer sampling intervals were associated with a reduced goodness of fit (Fig. 3b,c). The quality of the  $T_{\text{core}}$  estimate was strongly influenced by the length of the averaging interval (Fig. 3b,c). The accuracy of discrete  $T_{\text{core}}$  estimates increased consistently with longer averaging intervals in all five individual mice although the most pronounced increase occurred between averaging intervals of 10 and 60 min (Fig. 3b). The increasing accuracy by which progressively longer (> 60 min) discrete averaging intervals estimated the mean  $T_{\text{core}}$  over that same (long) interval (Fig. 3b) was however inherently coupled with a decreasing ability to describe  $T_{\text{core}}$  changes over time (Fig. S3). The optimisation of this trade-off between the accuracy of the average and describing  $T_{\text{core}}$  changes over time was done by sliding the averaging interval in 30 s steps to estimate a rolling average for  $T_{\text{core}}$  (Fig. 3c). This analysis demonstrated that averaging intervals of 30 or 60 min maximised the accuracy of the average and the description of the temporal changes in  $T_{\text{core}}$ . Furthermore, an averaging interval of 30 min resulted in a relationship between  $T_{\text{skin,max}}$  and  $T_{\text{core}}$  with an average slope close to 1 (Fig. S4). Based on these outcomes, we conclude that the optimal algorithm to estimate  $T_{\text{core}}$  based on  $T_{\text{skin}}$  measurements taken every second samples  $T_{\text{skin,max}}$  per 60 s and averages these values over 30 min intervals.

**Relationship between skin and core temperature.** Combining the  $T_{\text{skin}}$ -derived estimate obtained using the algorithm described above with the slope and intercept describing the linear relationship between  $T_{\text{skin,max}}$  and  $T_{\text{core}}$  optimised for each individual mouse resulted in an excellent description of  $T_{\text{core}}$  over the three-day test period (Fig. 4). Such an individualised optimisation does however require the implantation of a telemeter, thus negating the main benefit of using non-invasive thermal imaging to estimate  $T_{\text{core}}$ . Our goal here is to describe the average relationship between  $T_{\text{skin,max}}$  and  $T_{\text{core}}$  and assess whether these group-level parameters enable an adequate estimation of  $T_{\text{core}}$  based on  $T_{\text{skin}}$  measurements in individual mice.

The variance in the difference between  $T_{\text{core}}$  and  $T_{\text{skin,max}}$  was independent of  $T_{\text{core}}$  for all five mice (Fig. 5a), this temperature difference was only minimally influenced by the time of day (range of hourly averages: 4.7–5.1 °C,

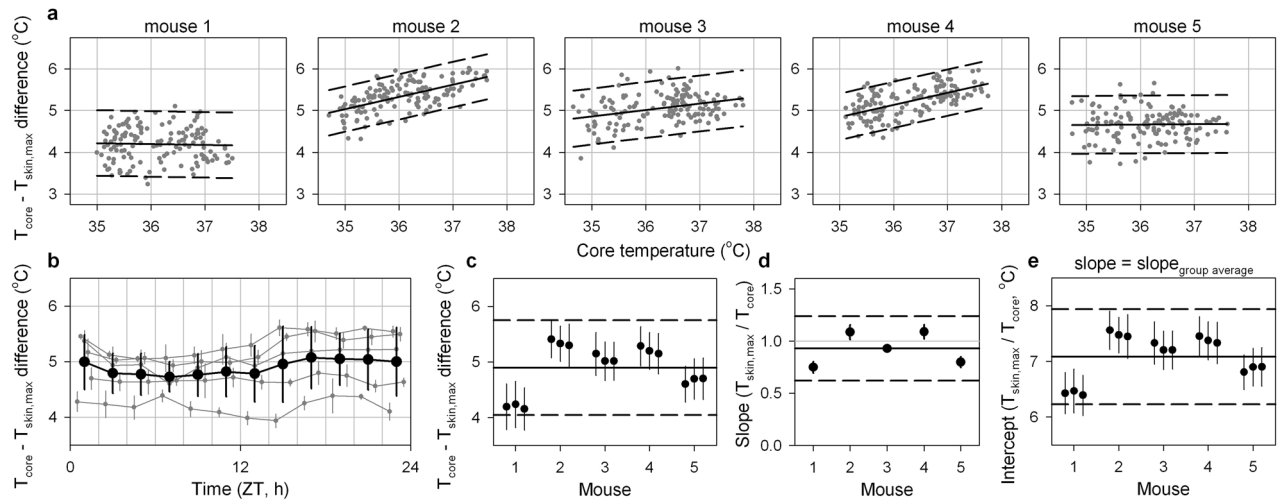


**Figure 5.** Core temperature ( $T_{\text{core}}$ ) estimation by continuous skin temperature ( $T_{\text{skin,max}}$ ) measurements; accuracy assessment. **(a)** Correlations of  $T_{\text{core}}$  with the difference between  $T_{\text{core}}$  and  $T_{\text{skin,max}}$  for all five mice. Comparisons are made between the average  $T_{\text{core}}$  per 30 min and the average of the maximum  $T_{\text{skin}}$  per minute over the same averaging interval. Solid lines represent the least-squares linear fit while dashed lines enclose the 2-standard-deviations area surrounding this fit. **(b)** The difference between  $T_{\text{core}}$  and  $T_{\text{skin,max}}$  was only marginally correlated with time of day ( $\sim 0.3$  °C,  $p < 0.0001$ ). Traces of individual mice (dark grey lines) are slightly offset on the x-axis to improve visibility. **(c)** The difference between  $T_{\text{core}}$  and  $T_{\text{skin,max}}$  on each of the three measurement days in all five mice. **(d)** The slope of the relationship between  $T_{\text{core}}$  and  $T_{\text{skin,max}}$  in all five mice. Mean and SD summarise the within-individual variance in slope between the three measurement days. **(e)** The intercept of the relationship between  $T_{\text{core}}$  and  $T_{\text{skin,max}}$  in all five mice. This assessment incorporated the group-average (0.93) as the slope for all mice. Within-individual variance in the difference between  $T_{\text{core}}$  and  $T_{\text{skin,max}}$  (**c**), slope (**d**) and intercept (**e**) was substantially lower than the between-individual variance. Solid lines in (**c–e**) represent the group mean while dashed lines enclose the 2-standard-deviations area surrounding this average. Error bars represent SD.

$p < 0.0001$ ; Fig. 5b), and the temperature difference was consistent across measurement days within each of the five mice (Fig. 5c). The difference between  $T_{\text{core}}$  and  $T_{\text{skin,max}}$  did not correlate with  $T_{\text{core}}$  in two of the five mice but in the other three mice a significant positive correlation was observed between  $T_{\text{core}}$  and the difference between  $T_{\text{core}}$  and  $T_{\text{skin,max}}$  (Fig. 5a). The relationship between  $T_{\text{core}}$  and the difference between  $T_{\text{core}}$  and  $T_{\text{skin,max}}$  was strongly dependent on the chosen sampling interval but not the averaging interval duration (Fig. S5A). Between-animal variance in this relationship was substantial, however, and precluded the selection of algorithm parameters that would prevent a correlation between  $T_{\text{core}}$  and the difference between  $T_{\text{core}}$  and  $T_{\text{skin,max}}$  in all mice (Fig. S5B). As noted above, the selected algorithm parameters resulted in a relationship between  $T_{\text{core}}$  and  $T_{\text{skin,max}}$  with a slope of  $\sim 1$  (Fig. 5d). When this average slope was used to estimate  $T_{\text{core}}$  based on  $T_{\text{skin,max}}$ , the observed residual difference between  $T_{\text{core}}$  and  $T_{\text{skin,max}}$  (intercept) was consistent between days within all mice, although the between-animal variance was substantial (Fig. 5e). Overall, the selected algorithm parameters (averaging maximum  $T_{\text{skin}}$  per 60 s over 30 min) resulted in an estimate of  $T_{\text{core}}$  that was highly consistent between days with equal variance at different  $T_{\text{core}}$  values, a minimised correlation between  $T_{\text{core}}$  and the difference between  $T_{\text{core}}$  and  $T_{\text{skin,max}}$ , and a relationship between  $T_{\text{skin,max}}$  and  $T_{\text{core}}$  with a slope and intercept of 0.93 and 7.1 °C respectively.

**Between-animal variability in the relationship between skin and core temperature.** A key aim of this study was to determine whether thermal imaging could be used to reliably estimate  $T_{\text{core}}$  non-invasively in freely-moving mice. To this end, it would be essential that  $T_{\text{core}}$  can be estimated without having to determine the relationship between  $T_{\text{core}}$  and  $T_{\text{skin,max}}$  for each individual animal. As a minimal assessment of this requirement, the group-average slope and intercept were used to estimate  $T_{\text{core}}$  based on  $T_{\text{skin,max}}$  in the five mice for which these group averages had been optimised. The use of the group average slope and intercept dramatically reduced the quality of  $T_{\text{core}}$  estimates in some of the mice (Fig. 6a) because it resulted in a systematic under- or overestimation of  $T_{\text{core}}$  (Fig. 6e) due to between-animal differences in slope and intercept. Changing of algorithm parameters could not further reduce the between-animal variance in slope and intercept (Figs. S4B, S6). As a result of the high between-animal variance in the relationship between  $T_{\text{core}}$  and  $T_{\text{skin,max}}$  observed in the current group of five mice,  $T_{\text{skin,max}}$  did not provide a reliable estimate of the absolute value of  $T_{\text{core}}$  in individual mice (systematic deviation range:  $-0.6$  to  $+0.9$  °C; Fig. 6b). To place these values in context, these deviations span approximately half the observed  $T_{\text{core}}$  range (3.1–3.8 °C; Fig. 4). Conversely, between-animal comparisons of absolute changes in  $T_{\text{core}}$  based on  $T_{\text{skin,max}}$  could be made with greater accuracy (systematic deviation range:  $-0.5$  to  $+0.5$  °C per 2.5 °C  $T_{\text{core}}$  change; Fig. 6c). Within-animal comparisons of relative changes in  $T_{\text{core}}$  could be estimated with the highest accuracy (systematic deviation: 0 °C, within-animal day-to-day intercept range: 0.2 °C, within-day intercept SD: 0.3–0.4 °C; Figs. 5e, 6d), thus demonstrating the utility of thermography for comparisons of relative  $T_{\text{skin}}$  changes between days (or treatments) within animals.

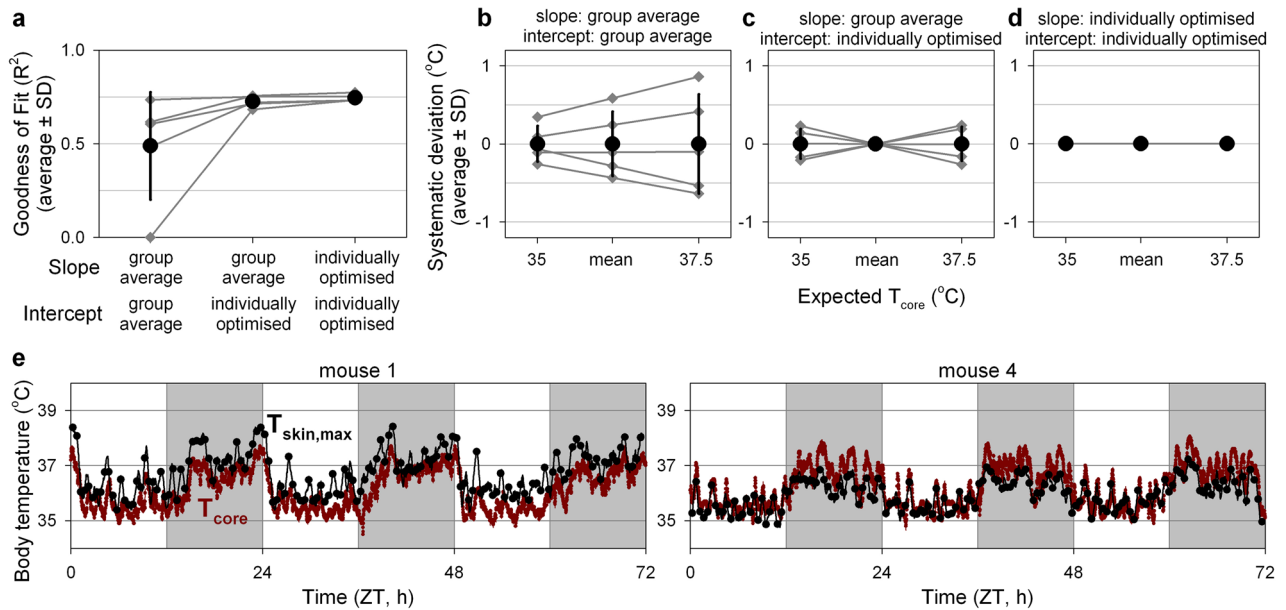


**Figure 6.** Between-animal variability in the relationship between  $T_{\text{skin,max}}$  and  $T_{\text{core}}$  limits utility of  $T_{\text{skin}}$ -derived estimates of  $T_{\text{core}}$ . **(a)** Goodness of fit associated with estimating  $T_{\text{core}}$  based on  $T_{\text{skin,max}}$  using group average or individually optimised values for the slope and/or intercept in individual mice (dark grey). Group averages are plotted in black. **(b–d)** Expected systematic temperature deviations at low, mean and high  $T_{\text{core}}$  for models using group averages or individually optimised values for the slope and/or intercept in individual mice (dark grey). Expected systematic deviations are calculated based on the difference between the group-average and individually-optimised slope and intercept for each individual mouse. Group averages are by definition 0, with greater SD values representing higher between-animal variation in the  $T_{\text{core}}$  estimation error. **(e)** Two representative examples of the measured  $T_{\text{core}}$  (red) and the estimated temperature based on  $T_{\text{skin,max}}$  (black) with group averages used as slope and intercept. Core temperature estimates based on  $T_{\text{skin}}$  are depicted as a rolling average (black line) and as discrete averages (black dots, 1 per 30 min). Day and night are represented by the white- and light-grey background, respectively. Error bars represent SD. ZT: Zeitgeber time.

**Estimating core body temperature during daily torpor.** Exposure to energetically challenging conditions (e.g. hunger, cold) induces energy saving strategies such as daily torpor in mice<sup>3</sup>. Here, food intake of three mice was restricted to a single daily meal consisting of ~70% of their ad libitum intake resulting in daily torpor bouts in all mice (duration: 4–8 h, minimum core temperature: 25–27 °C; Fig. 7a). In line with our findings in mice fed ad libitum, averaging  $T_{\text{skin,max}}$  per 60 s over a 30-min interval resulted in an accurate estimate of  $T_{\text{core}}$  (Fig. S7A–C) with comparable variance at different values of  $T_{\text{core}}$  (Fig. 7b). The relationship between  $T_{\text{core}}$  and  $T_{\text{skin,max}}$  had a slope that was consistently higher than that observed in homeothermic mice (Fig. S7D,E), reflecting an altered relationship between  $T_{\text{core}}$  and  $T_{\text{skin,max}}$  in mice under energetically challenging conditions. The difference between  $T_{\text{core}}$  and  $T_{\text{skin,max}}$  decreased linearly with lower values of  $T_{\text{core}}$  (Fig. 7b), thus complicating the  $T_{\text{skin}}$ -derived estimation of  $T_{\text{core}}$  (i.e. slope > 1). This correlation between  $T_{\text{core}}$  and the difference between  $T_{\text{core}}$  and  $T_{\text{skin,max}}$  could not be eliminated by altering algorithm parameters (Fig. S7F,G). Although the sample size was insufficient to reliably estimate between-animal variance in the relationship between  $T_{\text{core}}$  and  $T_{\text{skin,max}}$ , the observed difference in slopes in individual mice (range: 1.42–1.53, Fig. S8) would translate to systematic deviations of  $\pm 0.5$  °C between mice over the 10 °C temperature difference observed under these energetically challenging conditions. In line with our observations in ad libitum fed mice, the day-to-day within-animal variance in the relationship between  $T_{\text{core}}$  and  $T_{\text{skin,max}}$  was very limited (Fig. S7H–K). This demonstrated the utility of non-invasive continuous thermography measurements to perform within-animal comparisons of relative changes in  $T_{\text{core}}$  in mice during daily torpor.

## Discussion

Monitoring body temperature provides important information about the physiological and metabolic state of animals. Established techniques for measuring body temperature are associated with restraint stress, do not allow continuous recordings, and/or require complicated invasive surgery<sup>5</sup>. The use of infrared thermography has the potential to provide a non-invasive method to measure  $T_{\text{core}}$  but its own methodological limitations have to be taken into account<sup>5,6</sup>. Previous applications of non-contact  $T_{\text{skin}}$  measurements in biomedical research have been limited by the requirement that animals needed to be handled by the experimenter<sup>7–15</sup>, measurements were taken at a limited number of timepoints<sup>7,8,10–17</sup>, and/or measurements resulted in large datafiles requiring complex data analysis<sup>10,12,13,16–18</sup>. The present study developed, optimised and validated an algorithm that enables estimation of relative changes in  $T_{\text{core}}$  based on the continuous and non-invasive automated measurement of  $T_{\text{skin}}$  of mice housed at room temperature. The high variability in  $T_{\text{skin}}$  compared to  $T_{\text{core}}$  measurements (Fig. 1c) necessitates data processing to obtain a less-variable estimate of  $T_{\text{skin}}$ . Here we show that averaging the maximum  $T_{\text{skin}}$  per

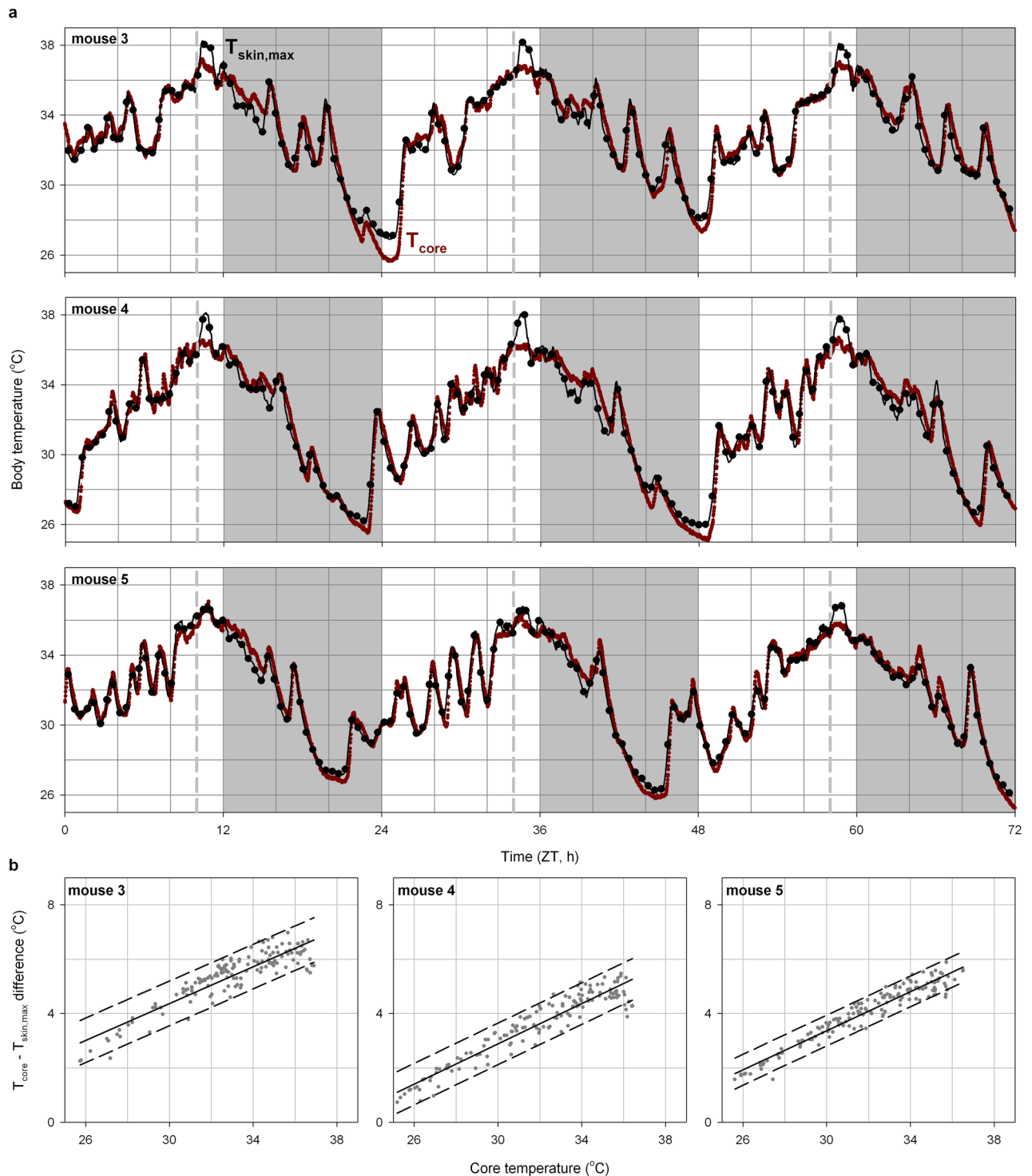


**Figure 7.** Body temperature during daily torpor in mice exposed to food restriction. **(a)** Three-day core temperature recordings measured directly ( $T_{\text{core}}$ , red) and estimated based on skin temperature ( $T_{\text{skin,max}}$ , black) of three mice during food restriction. Daily torpor was induced by chronic food restriction to  $\sim 70\%$  of ad libitum food intake. Food was provided daily, three hours before lights-off (dashed line). Day and night are represented by the white- and light-grey background, respectively. Skin temperature was calculated by averaging the maximum  $T_{\text{skin}}$  per minute over a 30-min interval. Slope and intercept describing the linear relationship between  $T_{\text{skin,max}}$  and  $T_{\text{core}}$  was optimised for each mouse individually. ZT: Zeitgeber time. **(b)** The difference between  $T_{\text{core}}$  and  $T_{\text{skin,max}}$  was strongly correlated with  $T_{\text{core}}$  in all three individual mice. Comparisons are made between the average  $T_{\text{core}}$  per 30 min and  $T_{\text{skin,max}}$  over the same averaging interval. Solid lines represent the least-squares linear fit while dashed lines enclose the 2-standard-deviations area surrounding this fit.

60 s over a 30 min interval ( $T_{\text{skin,max}}$ ) provides the most accurate estimate of  $T_{\text{core}}$ . High between-animal variability in the linear relationship between  $T_{\text{skin,max}}$  and  $T_{\text{core}}$  (i.e. slope and intercept) severely limits the accuracy of  $T_{\text{skin}}$  recordings as a measure of absolute  $T_{\text{core}}$ . Instead, because of the low day-to-day within-animal variability in the relationship between  $T_{\text{skin,max}}$  and  $T_{\text{core}}$ ,  $T_{\text{skin}}$  recordings provide an excellent tool to assess relative differences in  $T_{\text{core}}$  within individual animals.

Given the aforementioned strengths and limitations in estimating relative changes in  $T_{\text{core}}$  based on  $T_{\text{skin}}$ , this method provides an excellent tool to continuously monitor relative  $T_{\text{core}}$  changes in undisturbed, individually-housed, freely-moving mice. This was illustrated here by characterising the temporal fluctuations in body temperature throughout day and night as well as during daily torpor. The automated and continuous nature of the measurement and data processing steps presented here compare favourably with previous approaches using thermography to assess  $T_{\text{core}}$  changes<sup>10,12,13,16,17</sup>, albeit at the expense of accuracy of its absolute  $T_{\text{core}}$  estimate<sup>13,17</sup>. Although the inability to accurately estimate absolute  $T_{\text{core}}$  values compares negatively to telemeter implantation, this cost will often be outweighed by welfare, time and financial benefits associated with not having to perform surgery, especially in cases where (physiologically-relevant) changes in body temperature are the prime concern<sup>14,16,18</sup>. When used as a humane endpoint, body temperature is often compared to a reference value at a single timepoint<sup>8,11,14</sup>. Although such a between-animal comparison does not suit the current method, the continuous nature of its  $T_{\text{core}}$  estimate enables welfare decisions to be based on multiple characteristics such as the daily body temperature profile, its timing, and an individually calibrated set point. The requirement that animals are individually housed in open-top cages with reduced access to nesting materials (to ensure visibility of the animal) also provides a limitation of the current approach, although depending on the experimental paradigm this might be a worthwhile trade-off. Overall, we view the method presented here as a useful addition to a repertoire of different approaches to monitor body temperature<sup>5</sup>, that, depending on the specific research question, might provide benefits compared to other established techniques.

## Methods

All animal procedures were approved by the ACER AWERB of the University of Oxford and performed under a UK Home office license in accordance with all relevant laws and regulations. Five wildtype C57Bl6/J mice were implanted intraperitoneally with an Anipill temperature telemeter. Following post-operative recovery mice were housed at an ambient temperature of  $22 \pm 1$  °C in open-top cages, each positioned under a thermal camera.  $T_{\text{skin}}$  was measured every second by storing the temperature of the warmest pixel.  $T_{\text{core}}$  was measured every 30 s by the implanted Anipill. The quality of the  $T_{\text{skin}}$ -derived  $T_{\text{core}}$  estimate was optimised based on the goodness of fit and variance distribution associated with each combination of different summarising statistics (minimum, median, arithmetic mean, geometric mean and maximum), sampling intervals (1 s–10 min), and averaging intervals (30 s–12 h). The linear relationship (slope and intercept) between  $T_{\text{skin,max}}$  and  $T_{\text{core}}$  was assessed in 5 ad libitum fed mice and subsequently under energetically challenging conditions in 3 of these mice. Systematic deviations represent the difference between the estimated  $T_{\text{core}}$  calculated based on individually-optimised versus group-average based descriptions of the relevant relationship between  $T_{\text{skin,max}}$  and  $T_{\text{core}}$  for each of the animals and presented assessments. Extended methodological details are available in the *SI Methods* and software templates to calculate  $T_{\text{core}}$  estimates based on the methods described here have been uploaded to Figshare (10.6084/m9.figshare.12587909).

## Data availability

All raw data, scripts and outcomes per individual animal have been uploaded to Figshare (10.6084/m9.figshare.12587495). Software templates (MS Excel, SciLab, Matlab, R and Python) to estimate core body temperature based on skin temperature measurements can be downloaded from Figshare (10.6084/m9.figshare.12587909).

Received: 30 June 2020; Accepted: 13 November 2020

Published online: 26 November 2020

## References

- Evans, S. S., Repasky, E. A. & Fisher, D. T. Fever and the thermal regulation of immunity: The immune system feels the heat. *Nat. Rev. Immunol.* **15**(6), 335–349 (2015).
- Morrison, S. F. & Nakamura, K. Central mechanisms for thermoregulation. *Ann. Rev. Physiol.* **81**(1), 285–308 (2019).
- Geiser, F. Metabolic rate and body temperature reduction during hibernation and daily torpor. *Ann. Rev. Physiol.* **66**, 239–274 (2004).
- Herzog, C. J. *et al.* Chronic social instability stress in female rats: A potential animal model for female depression. *Neuroscience* **159**(3), 982–992 (2009).
- Meyer, C. W., Ootsuka, Y. & Romanovsky, A. A. Body temperature measurements for metabolic phenotyping in mice. *Front. Physiol.* **8**, 520 (2017).
- Tattersall, G. J. Infrared thermography: A non-invasive window into thermal physiology. *Comp. Biochem. Physiol. A. Mol. Integr. Physiol.* **202**, 78–98 (2016).
- Saegusa, Y. & Tabata, H. Usefulness of infrared thermometry in determining body temperature in mice. *J. Vet. Med. Sci.* **65**(12), 1365–1367 (2003).
- Warn, P. A. *et al.* Infrared body temperature measurement of mice as an early indicator of death in experimental fungal infections. *Lab. Anim.* **37**(2), 126–131 (2003).
- Bakken, G. S., Van Sant, M. J., Lynott, A. J. & Banta, M. R. Predicting small endotherm body temperatures from scalp temperatures. *J. Therm. Biol.* **30**(3), 221–228 (2005).
- Warner, A. *et al.* Inappropriate heat dissipation ignites brown fat thermogenesis in mice with a mutant thyroid hormone receptor  $\alpha 1$ . *Proc. Natl. Acad. Sci. USA* **110**(40), 16241–16246 (2013).



11. Adamson, T. W., Diaz-Arevalo, D., Gonzalez, T. M., Liu, X. & Kalkum, M. Hypothermic endpoint for an intranasal invasive pulmonary aspergillosis mouse model. *Comp. Med.* **63**(6), 477–481 (2013).
12. Crane, J. D., Mottillo, E. P., Famcombe, T. H., Morrison, K. M. & Steinberg, G. R. A standardized infrared imaging technique that specifically detects UCP1-mediated thermogenesis *in vivo*. *Mol. Metab.* **3**, 490–494 (2014).
13. Vogel, B. *et al.* Touch-free measurement of body temperature using close-up thermography of the ocular surface. *MethodsX* **3**, 407–416 (2016).
14. Mei, J. *et al.* Body temperature measurement in mice during acute illness: Implantable temperature transponder versus surface infrared thermometry. *Sci. Rep.* **8**, 3526 (2018).
15. Fiebig, K., Jourdan, T., Kock, M. H., Merle, R. & Thöne-Reineke, C. Evaluation of infrared thermography for temperature measurement in adult male NMRI nude mice. *J. Am. Assoc. Lab. Anim. Sci.* **57**(6), 715–724 (2018).
16. Gachkar, S. *et al.* 3-Iodothyronamine induces tail vasodilation through central action in male mice. *Endocrinology* **158**(6), 1977–1984 (2017).
17. Gjendal, K., Franco, N. H., Lund Ottesen, J., Bratbo Sørensen, D. & Olsson, I. A. S. Eye, body or tail? Thermography as a measure of stress in mice. *Physiol. Behav.* **196**, 135–143 (2018).
18. Hitrec, T. *et al.* Neural control of fasting-induced torpor in mice. *Sci. Rep.* **9**, 15462 (2019).

## Acknowledgements

We thank Cristina Blanco-Duque and Martin Kahn for assistance during surgery. VvdV and LEM are supported by Novo Nordisk Postdoctoral Fellowships run in partnership with the University of Oxford. CAP is funded by the Wellcome trust (WT106174/Z/14/Z). SLW is funded by a National Centre for the Replacement, Refinement and Reduction of Animals in Research (NC3Rs) PhD Studentship (NC/S001689/1). JK is supported by National Institutes of Health (NIH) grant R01 AA0278707. SNP is funded by the Biotechnology and Biological Sciences Research Council (BBSRC grants BB/I021086/1 and BB/S015817/1). The funders had no role in study design, data collection and analysis, decision to publish, or preparation of the manuscript.

## Author contributions

V.vdV., J.C., V.V.V. and S.N.P. designed experiments. C.A.P. developed, built and optimised measurement setups. L.A.B. performed pilot studies. V.vdV., S.L.W. and L.E.M. performed measurements. V.vdV. and J.K. performed analyses. V.vdV., S.K.E.T., L.B.K., A.S.F., T.S.W., T.Y. developed software templates. V.vdV. wrote the manuscript with input from all other authors.

## Competing interests

The authors declare no competing interests.

## Additional information

**Supplementary information** is available for this paper at <https://doi.org/10.1038/s41598-020-77786-5>.

**Correspondence** and requests for materials should be addressed to V.vdV. or S.N.P.

**Reprints and permissions information** is available at [www.nature.com/reprints](http://www.nature.com/reprints).

**Publisher's note** Springer Nature remains neutral with regard to jurisdictional claims in published maps and institutional affiliations.



**Open Access** This article is licensed under a Creative Commons Attribution 4.0 International License, which permits use, sharing, adaptation, distribution and reproduction in any medium or format, as long as you give appropriate credit to the original author(s) and the source, provide a link to the Creative Commons licence, and indicate if changes were made. The images or other third party material in this article are included in the article's Creative Commons licence, unless indicated otherwise in a credit line to the material. If material is not included in the article's Creative Commons licence and your intended use is not permitted by statutory regulation or exceeds the permitted use, you will need to obtain permission directly from the copyright holder. To view a copy of this licence, visit <http://creativecommons.org/licenses/by/4.0/>.

© The Author(s) 2020